IEEE Photonics Journal
An IEEE Photonics Society Publication

Open Access

Passively Q-Switched Ho,Pr:$LiLuF_4$ Laser at 2.95 μm Using $MoSe_2$

Volume 9, Number 5, October 2017

Zhengyu Yan
Guoqiang Li
Tao Li
Shengzhi Zhao
Kejian Yang
Shuaiyi Zhang
Mingqi Fan
Lei Guo
Baitao Zhang

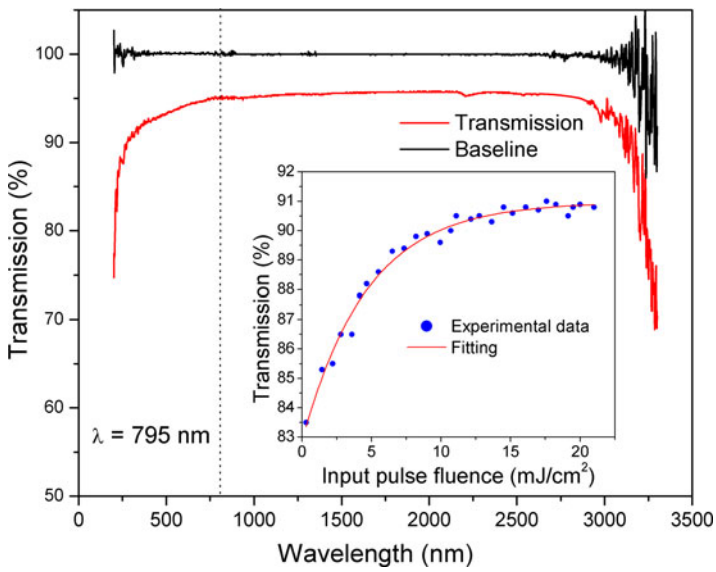

DOI: 10.1109/JPHOT.2017.2749328
1943-0655 © 2017 IEEE

Passively Q-Switched Ho,Pr:$LiLuF_4$ Laser at 2.95 μm Using $MoSe_2$

Zhengyu Yan,[1] Guoqiang Li,[1] Tao Li,[1] Shengzhi Zhao,[1] Kejian Yang,[1] Shuaiyi Zhang,[2] Mingqi Fan,[1] Lei Guo,[1] and Baitao Zhang[3]

[1]School of Information Science and Engineering and Shandong Provincial Key Laboratory of Laser Technology and Application, Shandong University, Jinan 250100, China
[2]Advanced Optoelectronic Materials and Technologies Engineering Laboratory of Shandong, Qingdao University of Science and Technology, Qingdao 266061, China
[3]State Key Laboratory of Crystal Materials, Institute of Crystal Materials, Shandong University, Jinan 250100, China

DOI:10.1109/JPHOT.2017.2749328

Manuscript received July 7, 2017; revised August 31, 2017; accepted September 2, 2017. Date of publication September 7, 2017; date of current version September 27, 2017. This work was supported in part by the National Key Research and Development Program of China under Grant 2016YFB1102201 and in part by the National Natural Science Foundation of China under Grants 61675116 and 61405101.
Corresponding author: Tao Li (e-mail: litao@sdu.edu.cn).

Abstract: In this letter, we report a diode-end-pumped continuous wave (CW) and passively Q-switched Ho,Pr:LLF laser at 2.95 μm. A maximum CW output power of 98 mW was achieved. The highest output power of 58 mW was radiated with a pulse duration of 818.8 ns and a repetition rate of 71.05 kHz. Even shorter pulse duration of 731.5 ns was obtained at a minor output coupler transmission.

Index Terms: Diode-pumped lasers, Q-switched lasers, solid state lasers.

1. Introduction

Mid-Infrared (mid-IR) lasers operating around 3.0 μm, which is well in the eyes of the security range, play an important role in medical, optical space communications, and remote sensing of atmosphere, since the strong water absorption ($\sim 10^4$ cm^{-1}) [1]–[3]. In addition, lasers within the range of 2.7 $\sim$ 3 μm can be used as a pumping source for optical parametric oscillators to achieve mid-IR lasers [4].

Similar to Er^{3+} ion [5], [6], laser operation at 2.9 μm can be realized by using holmium-doped mediums on the ${}^5I_6 \rightarrow {}^5I_7$ transition. The first Ho-doped ZBLAN fiber laser was achieved in 1990 by optical pumping at 640 nm, emitting within the wavelength from 2.83 to 2.95 μm [7]. However, it is hard to get an efficient laser operation with Ho-doped medium due to the depopulation of the upper level (${}^5I_6$), which is induced by the energy transfer upconversion (ETU) [8]–[11]. An efficient approach to enhance the laser transfer process in Ho^{3+} ions is the rare-earth sensitization. In fact, Pr^{3+} ion has been proved to be an outstanding co-doping ion to enhance the emission of Ho^{3+} at 2.9 μm through the energy transfer (ET) process of $Ho^{3+}:{}^5I_7 \rightarrow Pr^{3+}:{}^3F_2$ [12].

So far, Ho,Pr-doped fluoride fiber lasers operating around 2.9 μm have been studied by optical pumping at 1150 nm [10], [11], [13]. However, the high phonon energy of fluoride fiber decreases the population on $Ho:{}^5I_6$ through the multiphonon relaxation, limiting the output performances of the fiber lasers. In comparison with fluoride fiber, $LiLuF_4$ (LLF) crystal has several advantages: the lower multiphonon relaxation, which will result in long radiative and fluorescence lifetime of the level

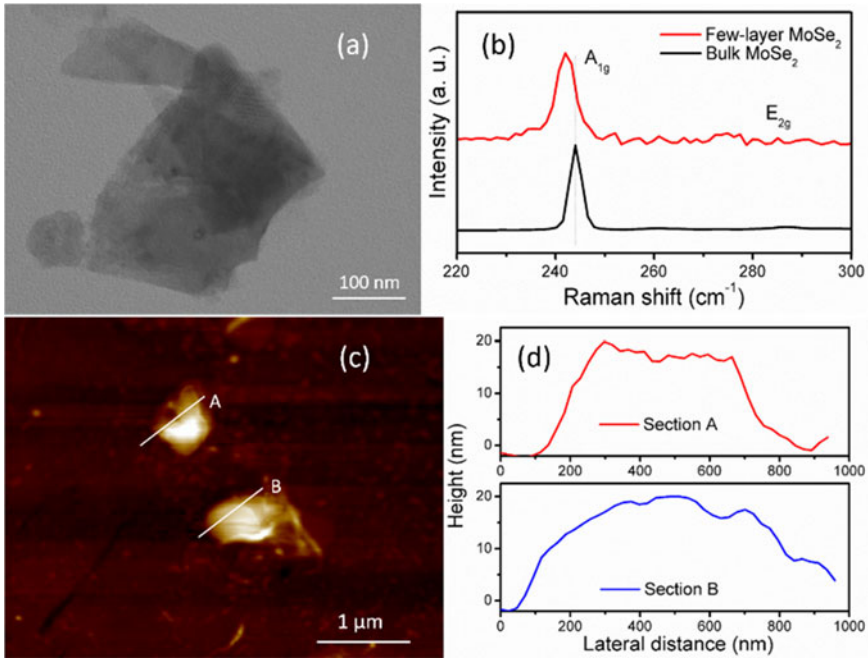

Fig. 1. (a) TEM image, (b) Raman spectra, (c) AFM image, and (d) height variation.

$^5I_6$ of Ho^{3+} ion; the inactive thermal dependence of refractive index, which will lead to the weak thermal lensing effect [14]. Those advantages make Ho,Pr:LLF to be a suitable host material for the 3 μm lasers.

In 2017, by employing monolayer graphene as saturable absorber, a diode-end-pumped CW and passively Q-switched Ho,Pr:LLF laser at 2.95 μm was demonstrated [15]. Diselenides (both of $MoSe_2$ and WSe_2) have outstanding semiconducting and non-linear optical properties [16], [17]. At present, the few-layer $MoSe_2$-SA has been successfully applied in fiber lasers at 1.06, 1.49–1.50, 1.56 and 1.92 μm, respectively [18], [19]. The saturable absorption property of $MoSe_2$ near 3 μm has not been reported, up to now.

In this letter, we fabricated a few-layer $MoSe_2$ film on an yttrium aluminum garnet (YAG) substrate. The nonlinear absorption properties of $MoSe_2$ at 2.95 μm were experimentally investigated. By employing the $MoSe_2$-SA in a plane-concave linear cavity, a stable Q-switched Ho,Pr:LLF laser operation at 2.95 μm was realized with the highest output power of 58 mW. The pulse repetition rate was 71.05 kHz with a pulse duration of 818.8 ns. The pulse energy was correspondingly calculated to be 0.82 μJ. The pulse duration can be further compressed to 731.5 ns by adopting an even small transmission of the output coupler.

2. Preparation and Characterization of $MoSe_2$ SA

The few-layer $MoSe_2$ film employed in our experiment was prepared by liquid-phase exfoliation (LPE) method [20]. The $MoSe_2$ dispersions was obtained by mixing bulk $MoSe_2$ with ethanol solvent and ultrasonicating for 12 h. After centrifugation at 2500 rpm for 15 min, the top two-third of the dispersions were decanted to another centrifuge tube for further processing.

In order to systematically characterize the $MoSe_2$ samples, transmission electron microscopy (TEM), Raman spectra and atomic force microscopy (AFM) were utilized. The TEM image of the $MoSe_2$ flake was depicted in Fig. 1(a), which obviously displays a 2D layered structure. By using a He-Ne laser at 632.8 nm, the Raman spectra was noted to prove the few-layer structure of $MoSe_2$, the results is shown in Fig. 1(b). One out-of-plane mode A_{1g} and one in-plane mode E_{2g} were detected. In contrast with the bulk curve, the A_{1g}-peak (244 cm^{-1} $\rightarrow$ 242 cm^{-1}) in the curve of

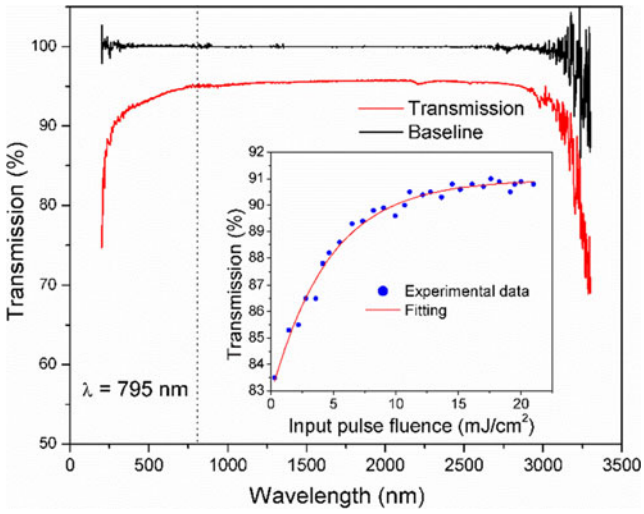

Fig. 2. Optical transmission spectrum of $MoSe_2$ film on a quartz substrate; insert: Nonlinear transmission of the YAG-based $MoSe_2$ film.

few-layer $MoSe_2$ indicates a redshift [21], [22]. The Raman shift confirms the few-layer structure was successfully exfoliated from the bulk $MoSe_2$ [19], [23]. Fig. 1(c) shows the AFM morphology of as-prepared $MoSe_2$-SA, which clearly reveals the $MoSe_2$ had been exfoliated to micron scale sheets. Fig. 1(d) shows a height profile of section A and B in Fig. 1(c). The height of $MoSe_2$ thin film is estimated to be between 16 and 20 nm corresponding to approximately 22 to 30 layers, assuming a mono-layer thickness is 0.9–1.0 nm [24], and 0.65 – 0.7 nm increase for each additional layer [25].

The optical transmission spectrum of the $MoSe_2$ flake was measured in the wavelength range from 200 nm to 3300 nm by an UV/VIS/NIR spectrophotometer (U-4100, Hitachi, Japan). A certain amount of supernatant was dripped upon a mid-infrared quartz plate with a dimensions of 60 mm $\times$ 20 mm, as the test sample. The measurement result was shown in Fig. 2, the black line is the baseline of the blank mid-infrared quartz. Normally, the $MoSe_2$ nanosheet possesses a narrow bandgap of 1.56 eV, corresponding to an absorption wavelength of 795 nm. However, the measurement result demonstrates a smooth wide absorption spectrum, which may induced by defect state or edge state saturable absorption [18], [26]. The absorption in the wavelength range from 800 nm to 3000 nm was measured to be $\sim$95.7%, which indicts a potential as a saturable absorber in 3 μm range.

A $MoSe_2$-SA was fabricated by dropping 5 μL supernatant onto a YAG substrate and drying at room temperature. The nonlinear optical absorption of the $MoSe_2$-SA was researched by a Q-switched laser at 2.84 μm. As shown in Fig. 2 (inset), the modulation depth of the $MoSe_2$-SA is $\sim$7.4%. The saturated transmission of the $MoSe_2$-SA amounted to be 90.9%. Considering the surface reflection of uncoated YAG substrate was measured to be 6.8%, the nonsaturable losses of the $MoSe_2$ film was estimated to be 2.3%. The saturation fluence of the $MoSe_2$ flake was calculated to be 3.6 mJ/cm^2.

3. Experiment Setup and Results

The schematic diagram of the $MoSe_2$ Q-switched laser is shown in Fig. 3. The pump source was a fiber-coupled laser diode emitting at 1150 nm. Through a coupling system (1:1), the pump light, coupled from a fiber with a spot diameter of 400 μm and a numerical aperture (NA) of 0.22, was focused into the gain medium. A 3.0 cm long plane-concave linear cavity was designed to realize efficient laser operation. The plane mirror M_1, anti-reflection (AR) coated at 1150 nm ($T > 95\%$) and high-reflection (HR) coated at 2.8–3.0 μm ($R > 99\%$), was used as input mirror. The concave

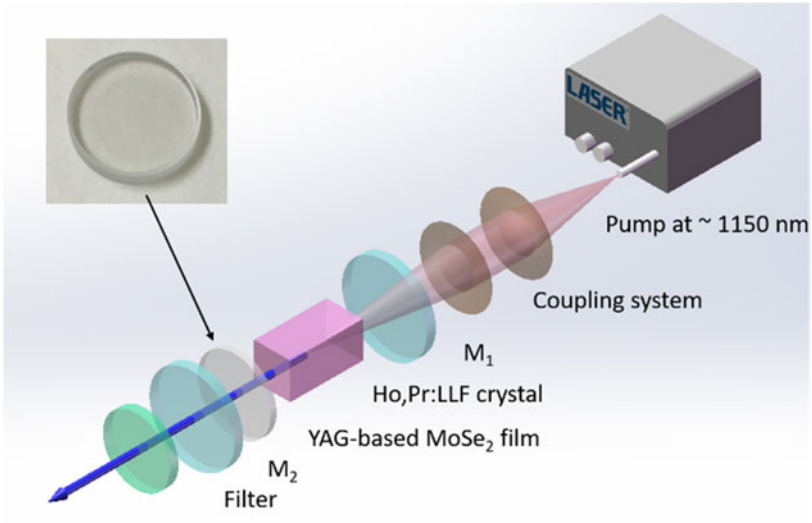

Fig. 3. Schematic diagram of the $MoSe_2$ Q-switched laser; insert: A YAG-based $MoSe_2$ film.

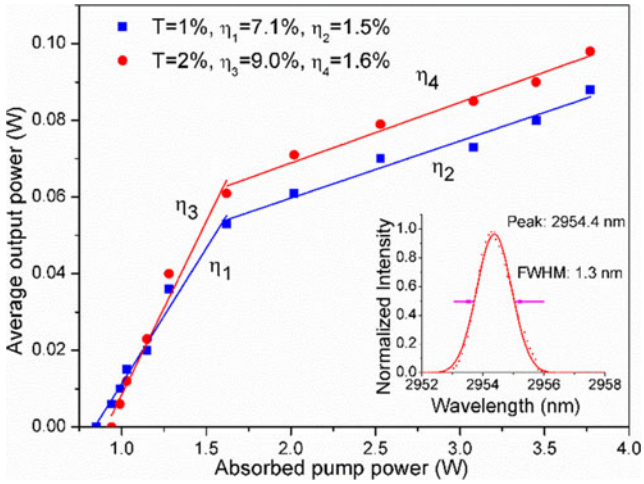

Fig. 4. Average output power versus absorbed pump power. The inset shows the output spectrum of the Ho,Pr:LLF laser.

mirrors M_2 ($r = 100$ mm) with different transmissions of 1% and 2% in the range of 2.8 – 3.0 μm were used as output couplers (OCs). The gain medium was an uncoated Ho,Pr:LLF crystal with Ho and Pr doping concentrations of 0.185 and 0.008 at. %. The crystal with a dimensions of 2 mm $\times$ 5 mm $\times$ 10 mm was wrapped by indium foil and mounted in a copper heat sink water-cooled to 12 °C. For blocking the remnant pump light, a filter was placed behind M_2. A PM100D power meter with a S314C power head (Thorlabs Inc., USA) was employed to measure the average output power. The laser output spectra were detected by an optical spectrum analyzer with a spectral resolution of 0.12 nm (MS3504i, SOL Instruments, Belarus).

The CW laser operations were studied first. Fig. 4 shows the output power versus the absorbed pump power. The threshold pump powers were 0.85 and 0.94 W at transmissions of T = 1% and 2%, respectively. Under the absorbed pump power of 3.77 W, a maximum output power of 98 mW was achieved at T = 2%. At the beginning, the output power linearly increased with the absorbed pump power, corresponding to a slope efficiency of 9.0%. When the absorbed pump power was increased more than 1.62 W, the slope efficiency dramatically decreased to a value of 1.6%. This phenomenon was similar to the Ho-doped fluoride fiber laser [27], which might be introduced by the ETU process of Ho^3+: $^5I_6 \rightarrow {}^5S_2$ [12], [27]. A higher concentration of Pr^{3+} ions might increase

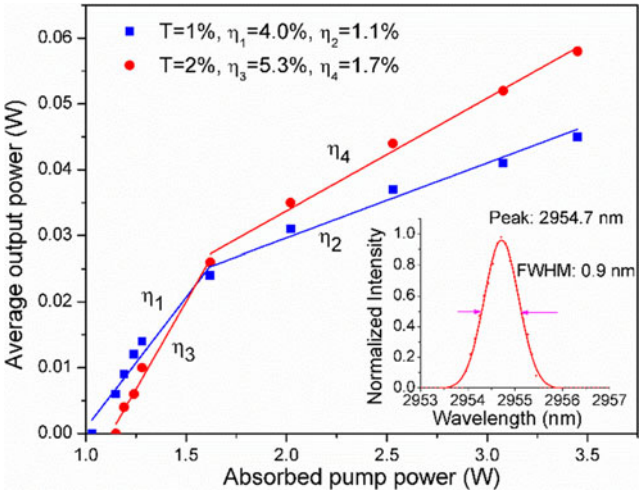

Fig. 5. Average output power of the $MoSe_2$ Q-switched Ho,Pr:LLF laser, and the inset displays the output spectrum.

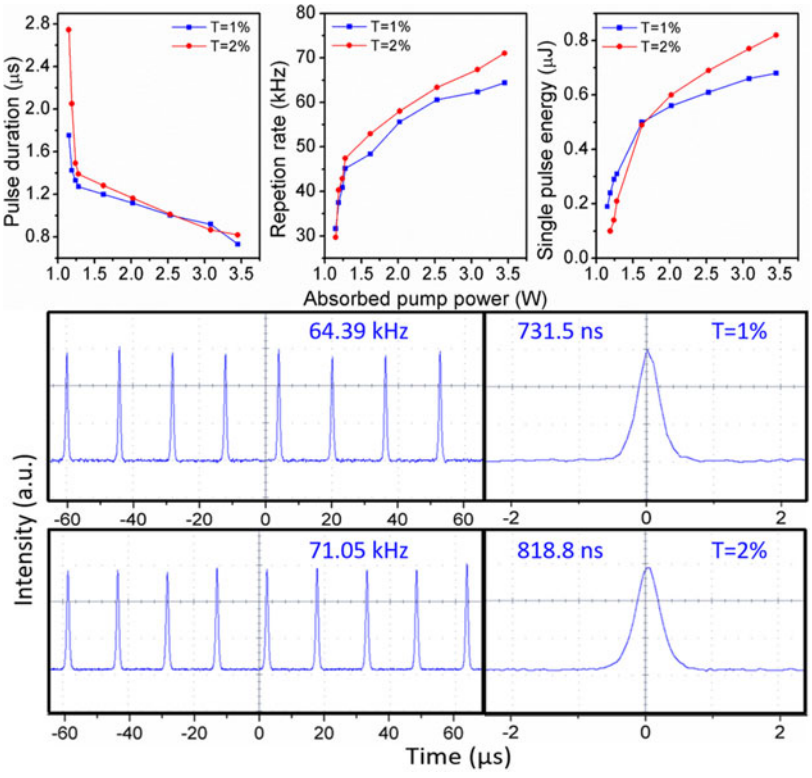

Fig. 6. Top: Performance of the pulse duration, repetition rate and single pulse energy versus absorbed pump power; bottom: Temporal traces of Q-switched pulse train.

the depopulation process of Ho^{3+}: $^5I_7$, leading to a higher efficiency [8].The center wavelength of the laser located at 2954.4 nm with a full width at half-maximum (FWHM) of 1.3 nm, as presented in Fig. 4 (inset).

Inserting the YAG-based $MoSe_2$-SA into the cavity, stable passively Q-switched laser operation was achieved. The relations between the average output power and the absorbed pump power are presented in Fig. 5. The maximum average output power of 58 mW was achieved at an absorbed

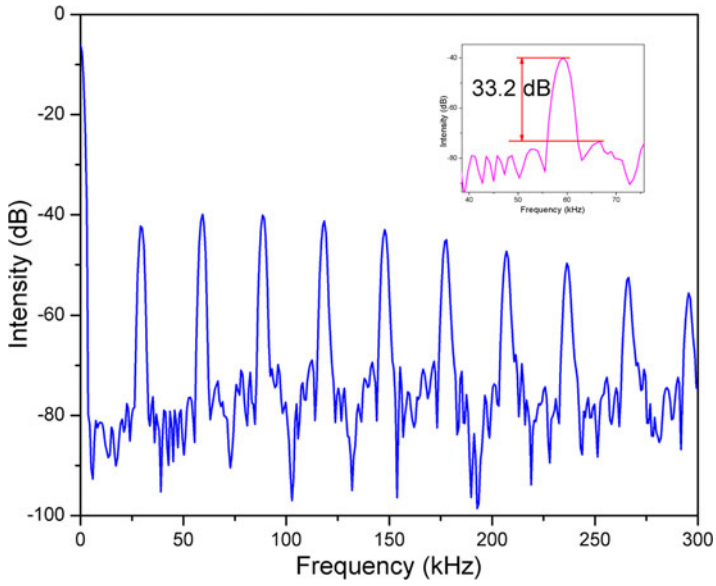

Fig. 7. RF spectrum of the $MoSe_2$ passively Q-switched pulses, insets show the spectrum at fundamental frequency.

pump power of 3.45 W. The increasing tendency was similar to the results acquired from the CW laser. The emission wavelength was measured to be ~2954.7 nm with a narrower FWHM of 0.9 nm, as shown in the inset of Fig. 5, which is caused by the insertion loss of $MoSe_2$-SA.

The laser pulse trains were detected by a fast HgCdTe IR detector with a response time of 1 ns (PVI-4TE-4, Vigo System S.A.) and recorded by a DPO 7104C digital phosphor oscilloscope (1 GHz bandwidth and 20 GS/s sampling rate, Tektronix Inc. USA). The relation of the pulse duration, pulse repetition rate and single pulse energy with the absorbed pump powers is shown in the top part of Fig. 6. Utilizing the output OC with T = 2%, the pulse repetition rate increased from 29.7 to 71.05 kHz with the absorbed pump power, while the pulse width changed from 2.746 μs to 818.8 ns in an opposite direction. The shortest pulse duration of 731.5 ns was obtained under an absorbed pump power of 3.45 W when a lower transmission of the output coupler was adopted with a value of T = 1%. Related to the passively Q-switched lasers with 2D SAs (such as WS_2, g-C_3N_4, black phosphorus and graphene), the pulse duration of 731.5 ns is among the shortest results [15], [28]–[31].

Under the maximum absorbed power of 3.45 W, the single pulse energy of 0.68 and 0.82 μJ were obtained at T = 1% and T = 2%, respectively. The bottom part of Fig. 6 shows the pulse trains and the temporal profiles of the shortest pulse. The pulse-to-pulse instability was found to be less than 10%. The radio frequency (RF) spectrum of the $MoSe_2$ passively Q-switched Ho,Pr:LiLuF$_4$ laser was recorded by a FieldFox RF Analyzer (4 GHz bandwidth, Agilent Technologies Inc. USA). As shown in Fig. 7, the signal-to-noise ratio is 33.2 dB, which indicates a fairly stable Q-switched operation.

4. Conclusion

In summary, a $MoSe_2$ SA based on YAG substrate was fabricated and a passively Q-switched Ho,Pr:LLF laser operation at 2.95 μm was correspondingly demonstrated. The laser generated a pulse as short as 731.5 ns. The highest average output power of 58 mW at a repetition rate of 71.05 kHz was achieved under an absorbed power of 3.45 W corresponding to a pulse energy of 0.82 μJ. Our results verified that the $MoSe_2$ possesses the potential for mid-IR laser modulation.

References

[1] M. Skorczakowski *et al.*, "Mid-infrared Q-switched Er:YAG laser for medical applications," *Laser Phys. Lett.*, vol. 7, no. 7, pp. 498–504, 2010.

[2] V. W. S. Chan, "Optical space communications," *IEEE J. Sel. Topics Quantum Electron.*, vol. 6, no. 6, pp. 959–975, Nov./Dec. 2000.

[3] T. M. Taczak and D. K. Killinger, "Development of a tumable, narrow-linewidth, CW 2.066-μm Ho:YLF laser for remote sensing of atmospheric CO_2 and H_20," *Appl. Opt.*, vol. 37, no. 36, pp. 8460–8476, 1998.

[4] K. L. Vodopyanov, F. Ganikhanov, J. P. Maffetone, I. Zwieback, and W. Ruderman, "$ZnGeP_2$ optical parametric oscillator with 3.8–12.4-μm tunability," *Opt. Lett.*, vol. 25, no. 11, pp. 841–843, 2000.

[5] T. Li, K. Beil, C. Kränkel, and G. Huber, "Efficient high-power continuous wave Er:Lu_2O_3 laser at 2.85 μm," *Opt. Lett.*, vol. 37, no. 13, pp. 2568–2570, 2012.

[6] M. Q. Fan *et al.*, "Graphitic C_3N_4 as a new saturable absorber for the mid-infrared spectral range," *Opt. Lett.*, vol. 42, no. 2, pp. 286–289, 2017.

[7] L. Wetenkamp, "Efficient CW operation of a 2.9 μm Ho^{3+}-doped fluorozirconate fibre laser pumped at 640 nm," *Electron. Lett.*, vol. 26, no. 13, pp. 883–884, 1990.

[8] S. D. Jackson, "Single-transverse-mode 2.5-W holmium-doped fluoride fiber laser operating at 2.86 μm," *Opt. Lett.*, vol. 29, no. 4, pp. 334–336, 2004.

[9] F. Z. Qamar, T. A. King, S. D. Jackson, and Y. H. Tsang, "Holmium,praseodymium-doped fluoride fiber laser operating near 2.87 μm and pumped with a Nd:YAG laser," *J. Lightw. Technol.*, vol. 23, no. 12, pp. 4315–4320, Dec. 2005.

[10] S. D. Jackson, F. Bugge, and G. Erbert, "Directly diode-pumped holmium fiber lasers," *Opt. Lett.*, vol. 32, no. 17, pp. 2496–2498, 2007.

[11] S. D. Jackson, "High-power and highly efficient diode-cladding-pumped holmium-doped fluoride fiber laser operating at 2.94 μm," *Opt. Lett.*, vol. 34, no. 15, pp. 2327–2329, 2009.

[12] P. X. Zhang, Y. Hang, and L. H. Zhang, "Deactivation effects of the lowest excited state of Ho^{3+} at 2.9 μm emission introduced by Pr^{3+} ions in $LiLuF_4$ crystal," *Opt. Lett.*, vol. 37, no. 24, pp. 5241–5243, 2012.

[13] T. Hu, D. D. Hudson, and S. D. Jackson, "Actively Q-switched 2.9 μm $Ho^{3+}Pr^{3+}$ -doped fluoride fiber laser," *Opt. Lett.*, vol. 37, no. 11, pp. 2145–2147, 2012.

[14] F. Cornacchia, A. Toncelli, and M. Tonelli, "2 μm lasers with fluride crystals: Research and development," *Prog. Quantum Electron.*, vol. 33, pp. 61–109, 2009.

[15] H. K. Nie *et al.*, "Diode-end pumped Ho,Pr:$LiLuF_4$ bulk laser at 2.95 μm," *Opt. Lett.* vol. 42, no. 4, pp. 699–702, 2017.

[16] Q. H. Wang, K. Kalantar-Zadeh, A. Kis, J. N. Coleman, and M. S. Strano, "Electronics and optoelectronics of two-dimensional transition metal dichalcogenides," *Nature Nanotechol.*, vol. 7, no. 11, pp. 699–712, 2012.

[17] B. H. Chen, X. Y. Zhang, K. Wu, H. Wang, J. Wang, and J. P. Chen, "Q-switched fiber laser based on transition metal dichalcogenides MoS_2, $MoSe_2$, WS_2, and WSe_2," *Opt. Exp.*, vol. 23, no. 20, pp. 26723–26737, 2015.

[18] R. I. Woodward *et al.*, "Wideband saturable absorption in few-layer molybdenum diselenide ($MoSe_2$) for Q-switching Yb-, Er- and Tm-doped fiber lasers," *Opt. Exp.*, vol. 23, no. 15, pp. 20051–20061, 2015.

[19] H. Ahmad *et al.*, "S-band Q-switched fiber laser using $MoSe_2$ saturable absorber," *Opt. Commun.*, vol. 382, pp. 93–98, 2017.

[20] J. N. Coleman *et al.*, "Two-dimensional nanosheets produced by liquid exfoliation of layered materials," *Science*, vol. 331, pp. 568–571, 2011.

[21] P. Tonndorf *et al.*, "Photoluminescence emission and Raman response of monolayer MoS_2, $MoSe_2$, and WSe_2," *Opt. Exp.*, vol. 21, no. 4, pp. 4908–4916, 2013.

[22] Z. Q. Luo *et al.*, "Nonlinear optical absorption of few-layer molybdenum diselenide ($MoSe_2$) for passively mode-locked soliton fiber laser [Invited]," *Photon. Res.*, vol. 3, no. 3, pp. A79–A86, 2015.

[23] J. C. Shaw *et al.*, "Chemical vapor deposition growth of monolayer $MoSe_2$ nanosheets," *Nono Res.*, vol. 7, no. 4, pp. 511–517, 2014.

[24] S. Tongay *et al.*, "Thermally driven crossover from indirect toward direct bandgap in 2D semiconductors: $MoSe_2$ versus MoS_2," *Nano Lett.*, vol. 12, pp. 5576–5580, 2012.

[25] Y. Zhang *et al.*, "Direct observation of the transition from indirect to direct bandgap in atomically thin epitaxial $MoSe_2$," *Nat. Nanotechnol.*, vol. 9, pp. 111–115, 2014.

[26] S. X. Wang *et al.*, "Broadband few-layer MoS_2 saturable absorbers," *Adv. Mater.*, vol. 26, pp. 3538–3544, 2014.

[27] S. D. Jackson, "Singly Ho^{3+} -doped fluoride fiber laser operating at 2.92 μm," *Electron. Lett.*, vol. 40, no. 22, pp. 1400–1401, 2004.

[28] L. Guo *et al.*, "Passively Q-switched Ho,Pr:$LiLuF_4$ bulk laser at 2.95 μm using WS_2 saturable absorbers," *Opt. Mater. Exp.*, vol. 7, no. 6, pp. 2090–2095, 2017.

[29] M. Fan *et al.*, "Passively Q-switched Ho,Pr:$LiLuF_4$ laser with graphitic carbon nitride nanosheet film," *Opt. Exp.*, vol. 25, no. 11, pp. 12796–12803, 2017.

[30] Z. Qin *et al.*, "Black phosphorus as saturable absorber for the Q-switched Er:ZBLAN fiber laser at 2.8 μm," *Opt. Exp.*, vol. 23, no. 19, pp. 24713–24718, 2015.

[31] C. Wei *et al.*, "Graphene Q-switched 2.78 μm Er^{3+} -doped fluoride fiber laser," *Opt. Lett.*, vol. 38, no. 17, pp. 3233–3236, 2013.